Available online at www.sciencedirect.com
ScienceDirect
Ceramics International 37 (2011) 3697–3702
CERAMICS INTERNATIONAL
www.elsevier.com/locate/ceramint

# The luminescence and structural characteristics of $Eu^{3+}$-doped $NaBaPO_4$ phosphor

Suyin Zhang [a], Donglei Wei [a], Rui Zhu [a], Yanlin Huang [a,*], Hyo Jin Seo [b,*]

[a] College of Chemistry, Chemical Engineering and Materials Science, Soochow University, Suzhou 215123, China
[b] Department of Physics, Pukyong National University, Busan 608-737, Republic of Korea

Received 9 May 2011; accepted 16 June 2011
Available online 23 June 2011

**Abstract**

$Eu^{3+}$-doped $NaBaPO_4$ was prepared by a high-temperature solid-state reaction. The phase formation was confirmed by X-ray powder diffraction measurements. The laser site-selective excitation and emission spectra have been investigated in the $^5D_0 \rightarrow {}^7F_0$ region by using a pulsed, tunable and narrowband dye laser. The excitation spectra corresponding to the $^7F_0 \rightarrow {}^5D_0$ transition consist of two transitions at 579.6 nm Eu(I) and 578.9 nm Eu(II), indicating the $Eu^{3+}$ ions occupy two crystallographic sites of $Ba^{2+}$ ions. The decay lifetimes of the two $Eu^{3+}$ sites were measured. Two crystallographic sites for $Eu^{3+}$ ions doped in $NaBaPO_4$ lattice were assigned from the luminescence characteristic and structure features. Meanwhile, the charge compensation mechanism of $Eu^{3+}$ doping in $NaBaPO_4$ was discussed.


*Keywords:* Phosphate; Structural occupation; Luminescence; Europium

## 1. Introduction

$Eu^{3+}$ has a simple electronic energy level scheme and its transitions are hypersensitive, i.e. they depend strongly on the chemical surroundings [1]. Because of these hypersensitive transitions, $Eu^{3+}$ has been used as a local structure probe in determining the microscopic symmetries of different sites available in various host lattices. Usually, the local structures, e.g., coordination numbers (CNs) and degree of distortion by defects, have an important inuence on the spectroscopic properties of $Eu^{3+}$ ions doped in a host [2]. As the most important emitter in the red region of the visible spectrum, $Eu^{3+}$ has gained considerable interest and been widely investigated to be the efficient red-emitting phosphors [3–10].

The phosphates with $ABPO_4$ formula ($A$ and $B$ are mono- and divalent cations, respectively) are in a large family of monophosphates with the different structure types strictly depending on the relative size of the $A$ and $B$ ions [11]. The variety in these structures makes it possible to tailor the physical and chemical properties of the $ABPO_4$ family materials. As an important family of luminescent materials, orthophosphates have been paid intense attention because of their excellent properties, e.g., the large band gap and the high absorption of $PO_4^{3-}$ in VUV region, moderate phonon energy, the high thermal and chemical stability, and the exceptional optical damage threshold [12].

Recently, RE-doped phosphors in $NaBaPO_4$ matrix have been extensively reported. $A$BaPO$_4$:Eu ($A$ = Na, K) [13] exhibit a mixed-valence europium state ($Eu^{3+}$ and $Eu^{2+}$) and the photoluminescence (PL) results show that the $NaBaPO_4$:Eu and $KBaPO_4$:Eu phosphors emit a strong blue light under UV excitation. $NaBaPO_4$:$Eu^{3+}$ [14] and $NaBaPO_4$:$Tb^{3+}$ [15] have been reported to be potential red-emitting and green-emitting W-LEDs phosphors, respectively. Upadeo and Moharil [16] investigated radiation-induced valence changes ($Eu^{3+} \rightarrow Eu^{2+}$ conversion) in Eu-doped $NaBaPO_4$. However, the structural occupation of $Eu^{3+}$ sites in $NaBaPO_4$ phosphor has not been reported in the present work yet.

In this work, $NaBaPO_4$:$Eu^{3+}$ was synthesized by a conventional high temperature solid-state reaction. The excitation and site-selective emission spectra have been investigated under pulsed dye laser excitation in the $^5D_0 \rightarrow {}^7F_0$ region of $Eu^{3+}$-doped $NaBaPO_4$. The site occupancy and the charge

* Corresponding authors.
*E-mail addresses:* Huang@suda.edu.cn (Y. Huang), hjseo@pknu.ac.kr (H.J. Seo).

0272-8842/$36.00 
doi:10.1016/j.ceramint.2011.06.032

compensation mechanism of $Eu^{3+}$ ions in the $NaBaPO_4$ lattices were discussed. This is helpful for the luminescence investigation of RE ions doped in this kind of phosphate host.

## 2. Experimental

The preparation of $NaBaPO_4$:$Eu^{3+}$ was carried out by solid state synthesis. The raw materials were high-purity (4 N) $Na_2CO_3$, $BaCO_3$, $NH_4H_2PO_4$ and $Eu_2O_3$. The doping level of $Eu^{3+}$ is 3.0 mol%. The starting materials with stoichiometric amounts were ground together in an agate mortar. The mixture was firstly heated up to 350 °C and kept at this temperature for 5 h. After a second homogenization in the mortar, the sample was heated up to 650 °C and kept at this temperature for 10 h. After that, the sample was mixed and heated at 900 °C for 10 h. The products were quenched to room temperature.

The X-ray diffraction (XRD) patterns were collected on a Rigaku D/Max-2000 diffractometer operating at 40 kV, 30 mA with Bragg–Brentano geometry by using Cu $K_\alpha$ radiation ($\lambda$ = 1.5418 Å) and analyzed using Jade-5.0 software. The optical excitation and emission spectra were recorded by a Perkin-Elmer LS-50B luminescence spectrometer and a Hitachi F-4500 fluorescence spectrophotometer.

For the excitation and site-selective emission measurements, the excitation source was a dye laser (Spectron Laser Sys. SL4000) pumped by the second harmonic (532 nm) of a pulsed Nd:YAG laser (Spectron Laser Sys. SL802G). The pulse energy was about 5 mJ with 10 Hz repetition rate and 5 ns duration. The samples were placed in a liquid helium flow cryostat for measurements at low temperatures. The luminescence was dispersed by a 75 cm monochromator (Acton Research Corp. Pro-750) and observed with a photomultiplier tube (Hamamatsu R928). Suitable filters were used to eliminate the intense laser scattering.

## 3. Results

### 3.1. The crystal phase formation

The XRD pattern of $NaBaPO_4$:$Eu^{3+}$ was compared with Joint Committee on Powder Diffraction Standards (JCPDS card No. 33-1210) (Fig. 1). By a comparison between them, the position and intensity of the main peaks are the same. No impurity lines were observed, and all the reflections could be well indexed to a $NaBaPO_4$ single phase. The lattice parameters of the sample were fitted by Jade.5.0 program to be $a = b = 5.612$ Å, $c = 7.24$ Å, $V = 197.5$ Å$^3$ and $Z = 2$. These results well agree with the reported data of pure $NaBaPO_4$, i.e. $a = b = 5.622$ Å, $c = 7.259$ Å, $V = 198.7$ Å$^3$ [17].

Fig. 2 presents the three-dimensional framework of $NaBaPO_4$ crystal structure with space group $P\bar{3}m1$. The schemes were modeled using the Diamond Crystal and Molecular Structure Visualization software on the basis of the atomic coordinates data reported in Ref. [17]. The structure is isotypic with that of glaserite. There are three different cation sites in the three-dimensional framework. Na and Ba lie at sites of 3 *m* symmetry and are coordinated to 6 and 12 oxygen atoms,

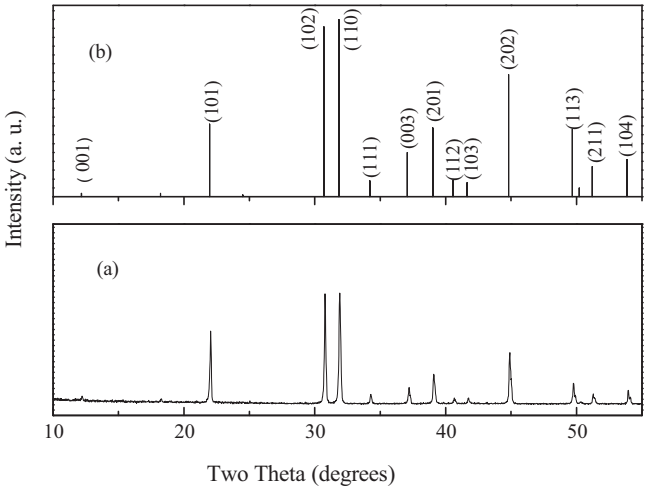


Fig. 1. XRD patterns of $NaBaPO_4$:$Eu^{3+}$ (a) and JCPDs card No. 33-1210 (b).

respectively. The remaining cation site has 3 *m* symmetry, a coordination number of 10, and contains equal amounts of $Na^+$ and $Ba^{2+}$ [18]. $Na^+$, $Ba^{2+}$ and *Y* cation ions alternate in the chains along the *c* axis as shown in Fig. 2. The main characteristic of $NaBaPO_4$ structure consists in a statistical occupation of the *Y* sites by $Na^+$ or $Ba^{2+}$ [17].

### 3.2. Photoluminescence spectra

The photoluminescence excitation and emission spectra of $NaBaPO_4$:$Eu^{3+}$ 3.0 mol% are shown in Fig. 3. In the excitation spectrum (Fig. 3(a)), the broad band ranging from 200 to 300 nm with a maximum at 256 nm are the charge transfer (CT) transition from the 2*p* orbital of the $O^{2-}$ to the 4*f* orbital of the $Eu^{3+}$. The dominated sharp lines in the wavelength region of 350–500 nm are from the f–f transitions within $4f^9$ configuration of $Eu^{3+}$ ions. Obviously, the excitation spectrum (Fig. 3(a)) indicates that $NaBaPO_4$:$Eu^{3+}$ 3.0 mol% can be efficiently excited by the radiation of near UV-emitting InGaN based LED chips (around 400 nm).

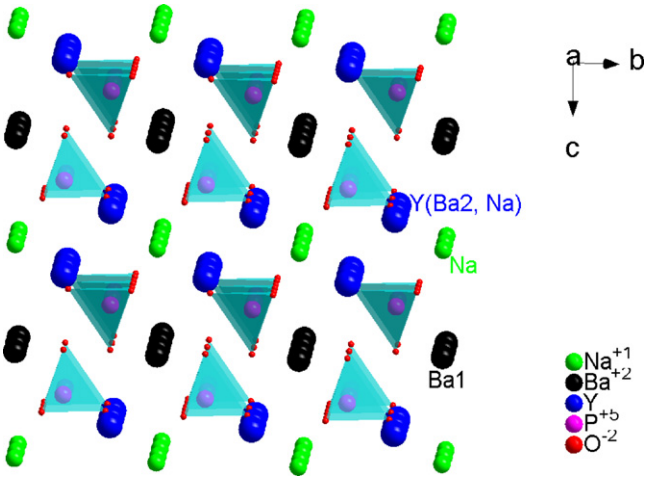


Fig. 2. Schematic crystal structures of two unit cells, revealing a well-ordered array of Na, Ba1, and *Y* (Ba2, Na) atoms.

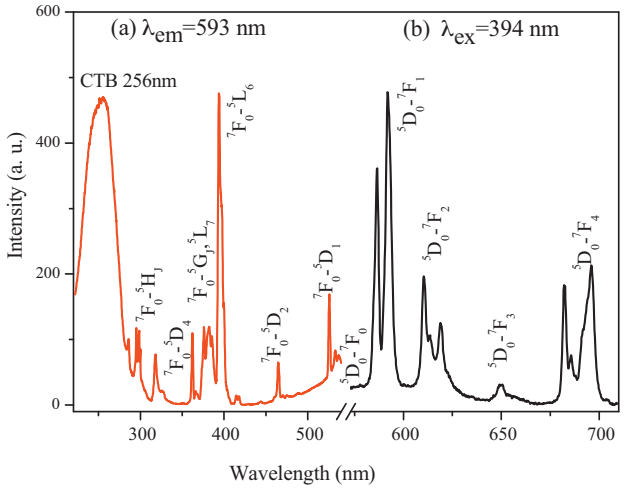


Fig. 3. The photoluminescence excitation and emission spectra of $NaBaPO_4:Eu^{3+}$.

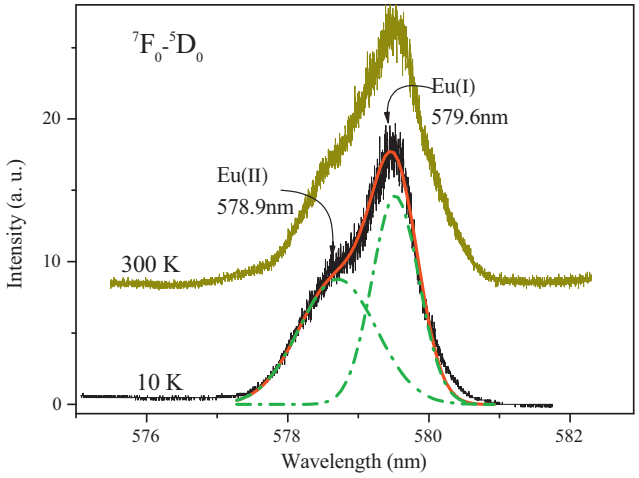


Fig. 4. The excitation spectra for $^7F_0 \rightarrow {}^5D_0$ transition of $Eu^{3+}$ in $NaBaPO_4:Eu^{3+}$ at 10 K and 300 K by monitoring the total luminescence, of which the spectrum at 10 K was deconvoluted to two Gassian components.

The emission spectra under the excitation of 394 nm are shown in Fig. 3(b). The spectra consist of a number of sharp lines ranging from 575 to 710 nm, which are associated with the transitions from the excited state $^5D_0$ to $^7F_J$ ($J = 0, 1, 2, 3$ and 4) levels of $Eu^{3+}$. The red emission at 612 nm is an electric dipole transition, while the orange emission range at 593 nm is a typical magnetic dipole transition. The emission spectra are dominated by the transitions of $^5D_0 \rightarrow {}^7F_1$. According to the Judd–Ofelt theory, the magnetic dipole transition is permitted. However, the electric dipole transition is allowed only when the europium ion occupies a site without an inversion center and the intensity is significantly affected by the symmetry in local environments around $Eu^{3+}$ ions. If the $Eu^{3+}$ ions occupy an inversion symmetry site, the o-red emission, magnetic transition $^5D_0 \rightarrow {}^7F_1$ is the dominant transition. On the contrary, the electric dipole transition $^5D_0 \rightarrow {}^7F_2$ is the dominant transition [19].

### 3.3. The excitation spectra of $^7F_0 \rightarrow {}^5D_0$ transition

$Eu^{3+}$ ($4f^6$ configuration) is largely used as a probe of the surrounding symmetry because the emission and excitation lines between $^5D_0$ and $^7F_0$ levels are the non-degenerate and they cannot be split by a crystal field surrounding the $Eu^{3+}$ions. This reveals the presence of crystallographic nonequivalent sites in a given host matrix [2]. In order to examine the site-distributions of $Eu^{3+}$ ions in $NaBaPO_4$, the excitation spectra and site-selective emission spectra were measured. Fig. 4 shows the excitation spectra corresponding to the $^7F_0 \rightarrow {}^5D_0$ transition at 10 K and 300 K obtained by monitoring the total luminescence from $NaBaPO_4:Eu^{3+}$.

It is found that the excitation band appears to be asymmetric on the short wavelength side in Fig. 4, this implies that $Eu^{3+}$ ions occupy more than one site in the $NaBaPO_4$ lattice. To investigate the relation between the coordinative environment and photoluminescence properties of $Eu^{3+}$ ions, the excitation spectrum at 10 K was deconvoluted into two Gaussian components peaked at the low-energy component of 579.6 nm (referred to as Eu(I)) and the high-energy component of 578.9 nm (referred to as Eu(II)), as shown in Fig. 4. No other line corresponding to $^7F_0 \rightarrow {}^5D_0$ transition was detected. It can be seen that the occupation probability of the major site Eu(I) is dominant. The minor site Eu(II) is weakly occupied due to its weak excitation intensity. The observation of two excitation bands is in agreement with the results of two crystallographic sites available in $NaBaPO_4$ [17,18]. Tang and Chen [13] recently have reported that there are two $Eu^{2+}$ emission bands in $NaBaPO_4$, which can be ascribed to $Eu^{2+}$ ions on the two crystallographic sites.

### 3.4. The site-selective emission spectra

The site-selective emission spectra under the Eu(I)- and Eu(II)-line excitations at 10 and 300 K for $NaBaPO_4:Eu^{3+}$ are shown in Fig. 5. The different emission spectra due to the $^5D_0 \rightarrow {}^7F_J$ ($J = 1$, 2, 3 and 4) transitions were observed. According to the emission spectra at 10 K, the wavelengths and energies of the $^5D_0 \rightarrow {}^7F_J$ ($J = 0$, 1, 2, 3 and 4) transitions within each $Eu^{3+}$ site were derived and listed in Table 1. It can be seen that the emission intensity of $^5D_0 \rightarrow {}^7F_1$ transition under the Eu(I)-line excitation is stronger than that of $^5D_0 \rightarrow {}^7F_2$ transition in Fig. 5(a), however, the emission intensity of $^5D_0 \rightarrow {}^7F_1$ transition under the Eu(II)-line excitation is weaker than that of $^5D_0 \rightarrow {}^7F_2$ transition in Fig. 5(b). The intensity ratio of $R = I(^5D_0 \rightarrow {}^7F_2)/I(^5D_0 \rightarrow {}^7F_1)$ is a measure of $Eu^{3+}$ ion's site symmetry. A higher symmetry of the crystal field around $Eu^{3+}$ will result in a smaller value [2].

In the site-selective emission spectra of Eu(I) site in Fig. 5(a), the magnetic-dipole transition $^5D_0 \rightarrow {}^7F_1$ is the most prominent group, while the $^5D_0 \rightarrow {}^7F_2$ transitions are very weaker. By means of calculation, the intensity ratios $R$ are 0.32 and 0.51 at 10 K and 300 K, respectively. However, the $R$ are 3.33 and 3.14 at 10 K and 300 K respectively in the site-selective emission spectra of Eu(II) site in Fig. 5(b). Obviously, the intensity ratios $R$ values in Eu(I) site excitation are very smaller than that in Eu(II) site. So the symmetry of Eu(I) site could be higher than that of Eu(II) site.

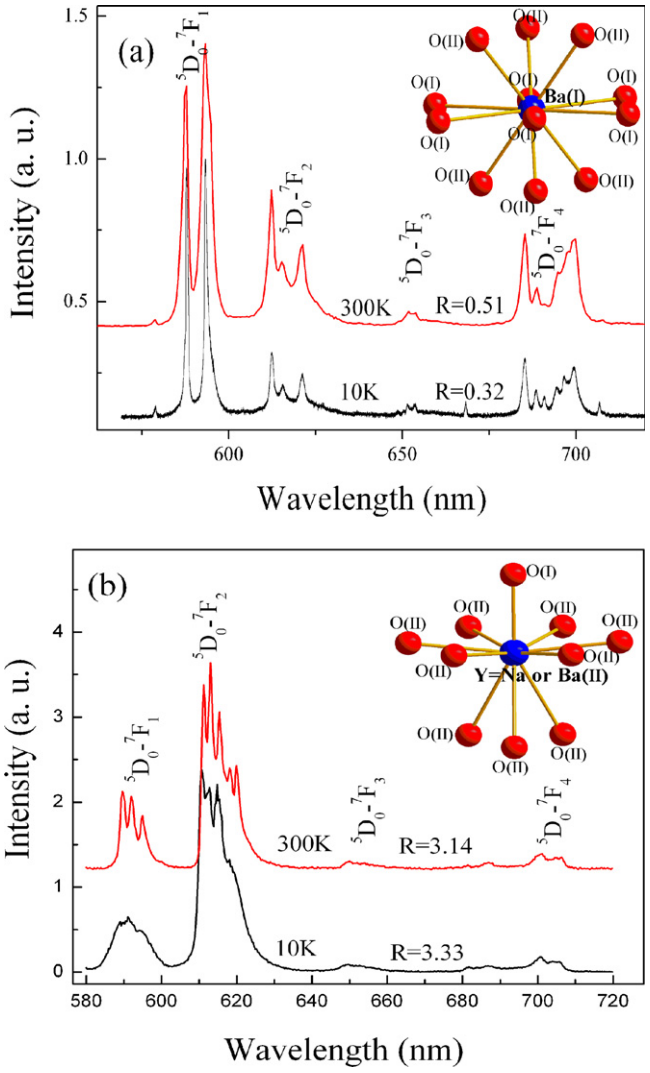


Fig. 5. The emission spectra of $^5D_0 \rightarrow {}^7F_J$ ($J$ = 1, 2, 3 and 4) under the site-selective excitation into $Eu^{3+}$(I) at 579.6 nm (a) and $Eu^{3+}$(II) at 578.9 nm (b) at 10 K and 300 K. The $R$ values in figure are the integrated intensity ratio of ($^5D_0 \rightarrow {}^7F_2$)/($^5D_0 \rightarrow {}^7F_1$) and the insets represent crystal structures of Ba(I) (a) and Ba(II) (b).

Inset in Fig. 5(a) exhibits the crystallographic structure of $Ba^{2+}$ site in $NaBaPO_4$. It is noticed that $Ba^{2+}$ shares six O(I) and six O(II). The six apical oxygen atoms, O(I)s, are nearly coplanar and they together with the $Ba^{2+}$ are said to lie in the equatorial plane of this cation. It is found that the distances of Ba(I)–O(I), and Ba(I)–O(II) are 3.247 and 2.788 Å, respectively, so the mean Ba(I)–O distance is 3.018 Å. The crystallographic structure of $Y$ site, which is occupied by equal amounts of $Na^+$ or $Ba^{2+}$, is illustrated in the inset of Fig. 5(b). According to calculation, the bond lengths of Ba(II)-six O(II) and Ba(II)-other three O(II) are 2.839 and 3.018 Å, respectively, while the distance of Ba(II)–O(I) is 2.416 Å, as a result, the average Ba(II)–O distance is 2.850 Å. So there are two different sites that 12 and 10 coordination occupied by Ba(I) and Ba(II) respectively in $NaBaPO_4$ lattices. This is clearly indicated that the symmetry of Ba (I) site is supposed to be higher than that of Ba (II) site. Based on the effective ionic radii of cations with different coordination numbers, it could be proposed that $Eu^{3+}$ ions occupy preferably the $Ba^{2+}$ sites. So this undoubtedly points to that the dominated Eu(I) is from the $Eu^{3+}$ ion that substitutes the Ba(I) while the Eu(II) is supposed to occupy the site of the Ba(II). It is in accord with the emission spectra of $Eu^{3+}$ ions in $NaBaPO_4$ lattices.

Table 1
The emission wavelengths (nm) and wave numbers ($cm^{-1}$) corresponding to the $^5D_0 \rightarrow {}^7F_J$ ($J$ = 1, 2, 3 and 4) transitions at 10 K in $NaBaPO_4$:$Eu^{3+}$.

| Transitions | Sites | | | |
|---|---|---|---|---|
| | Eu(I) | | Eu(II) | |
| | (nm) | ($cm^{-1}$) | (nm) | ($cm^{-1}$) |
| $^5D_0 \rightarrow {}^7F_0$ | 579.52 | 17,256 | 578.9 | 17,274 |
| $^5D_0 \rightarrow {}^7F_1$ | 588.3 | 16,998 | 589.6 | 16,961 |
| | 593.3 | 16,855 | 592 | 16,892 |
| | | | 595 | 16,807 |
| $^5D_0 \rightarrow {}^7F_2$ | 612.3 | 16,332 | 611.2 | 16,361 |
| | 615.5 | 16,247 | 613 | 16,313 |
| | 621.1 | 16,100 | 615.4 | 16,250 |
| | | | 618.1 | 16,179 |
| | | | 619.9 | 16,132 |
| $^5D_0 \rightarrow {}^7F_3$ | 648.7 | 15,415 | 649 | 15,408 |
| | 650.3 | 15,378 | 649.9 | 15,387 |
| | 651.5 | 15,349 | 650.5 | 15,373 |
| | 653.5 | 15,302 | 652 | 15,337 |
| | 653.8 | 15,295 | 654.1 | 15,288 |
| | 668.4 | 14,961 | 654.7 | 15,274 |
| $^5D_0 \rightarrow {}^7F_4$ | 685.3 | 14,592 | 685.9 | 14,579 |
| | 688.5 | 14,524 | 686.8 | 14,560 |
| | 691 | 14,472 | 688 | 14,535 |
| | 694.5 | 14,399 | 699.4 | 14,298 |
| | 696.8 | 14,351 | 701.2 | 14,261 |
| | 699.6 | 14,294 | 704.5 | 14,194 |
| | 706.7 | 14,150 | 706.3 | 14,158 |

### 3.5. The luminescence decay

The luminescence decay curves of the $^5D_0$ emission after the Eu(I)- and Eu(II)-line excitations at different temperatures were measured. The typical decay curves at 10 K and 300 K are shown in Fig. 6. It can be seen that the decay curves are single exponential. The exponential decay curve can be fitted into a single exponential function as:

$$I = I_0 \exp\left[\frac{-t}{\tau}\right] \quad (1)$$

where $I_0$ is the initial emission intensity for $t$ = 0, $\tau$ is lifetime. The luminescence lifetimes of the $Eu^{3+}$ ions are calculated as a function of temperature. The $^5D_0$ luminescence lifetimes are 2.31 and 2.01 ms in Eu(I) and Eu(II) site at 10 K, respectively. However, the $^5D_0$ decay time of $Eu^{3+}$ ions in Eu(I) and Eu (II) site is 2.11 ms and 1.49 ms at 300 K, respectively. It is found that with the temperature increasing; the lifetimes drop gradually, presenting a typical temperature quenching behavior. In addition, the lifetimes in Eu(I) site are longer than that in Eu(II) site. This agrees well with the excitation spectra intensity of $Eu^{3+}$ ions in the two sites as shown in Fig. 4.

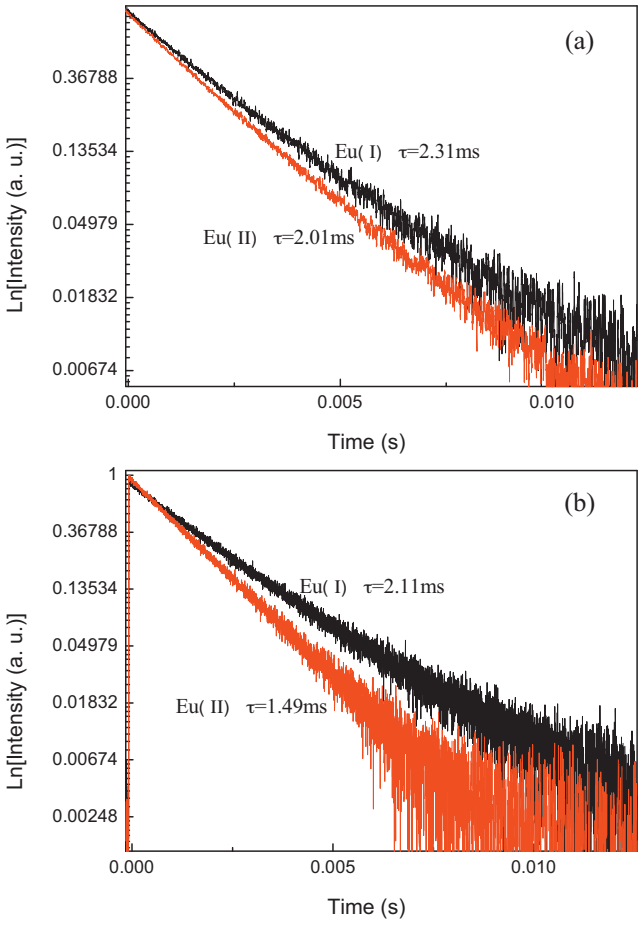


Fig. 6. The luminescence decay curves of $NaBaPO_4$:$Eu^{3+}$ at (a) 10 and (b) 300 K after the excitation of 579.6 nm by monitoring $^5D_0 \rightarrow {}^7F_1$ emission of 592 nm in Eu(I) and after the excitation of 578.9 nm by monitoring 612 nm in Eu(II).

## 4. Discussions

The uorescence spectroscopy of $Eu^{3+}$ can give information about the sites occupied by $Eu^{3+}$ in the lattices because each $Eu^{3+}$ center with different crystal eld symmetry possesses a unique optical transition in the $^7F_0 \rightarrow {}^5D_0$ excitation spectrum. The energy levels of $Eu^{3+}$ centers are very sensitive to the local environment of the corresponding cation [2]. So the local structure environments around $Eu^{3+}$ ions have an important inuence on its spectroscopic properties in a host. The following discussions were about the luminescence and site occupancy of $Eu^{3+}$ ions in $NaBaPO_4$.

First, site symmetry also inuences the $^5D_0$–$^7F_2$/$^5D_0$–$^7F_1$ intensity ratio, which corresponds to an ''asymmetry'' parameter. The $^5D_0$–$^7F_2$/$^5D_0$–$^7F_1$ intensity ratio increases when the contribution of the electrical dipolar interaction in the transition probability increases. This effect is related to distortion occurring in the europium surrounding [20]. As discussed above, the intensity ratios $R$ is 0.32 at 10 K in the site-selective emission spectra of Eu(I) site in Fig. 5(a), however, the $R$ is 3.33 at 10 K for Eu(II) site in Fig. 5(b). The site Eu(I) with smaller values of the $(^5D_0 \rightarrow {}^7F_2)/(^5D_0 \rightarrow {}^7F_1)$ emission ratio, presents therefore more symmetrical than the site Eu(II). Based on the effective ionic radii of cations with different coordination numbers, it could be proposed that $Eu^{3+}$ ions occupy preferably the $Ba^{2+}$ sites. This undoubtedly points to that the dominated Eu(I) is from the $Eu^{3+}$ ion that substitutes the Ba(I) while the Eu(II) is supposed to occupy the site of the Ba(II).

Secondly, the splitting of the $^7F_1$ or $^7F_2$ levels is characteristic of the crystal eld strength [21]. As the Eu–O mean distance decreases, the crystal eld as well as the splitting of the $^7F_1$ and $^7F_2$ energy levels increase [20]. As we know, considering the $2J + 1$ components for the $Eu^{3+}$ in the crystal field, the maximum splitting number of the transition lines for $^5D_0 \rightarrow {}^7F_J$ ($J = 0, 1, 2$) were 1, 3, 5, respectively, for each site. From Table 1, for resonant excitations with the site Eu(I) in Fig. 5(a), the spectra has 2 and 3 emission lines, for $^5D_0 \rightarrow {}^7F_1$ and $^5D_0 \rightarrow {}^7F_2$ transitions, respectively. Under site-selective excitation into site Eu(II), emission lines for $^5D_0 \rightarrow {}^7F_1$ and $^5D_0 \rightarrow {}^7F_2$ transitions are 3 and 5, respectively. This means that the symmetry of the crystal-field in site Eu(I) is higher than that of site Eu(II). Such emission spectra are consistent with the structure description. This indicates that $Eu^{3+}$ in site Eu(I) should occupy the position Ba(I) with $C_2$ symmetry. This conclusion is supported by the distance of Eu(I)–O (Ba(I)–O) longer than that of Eu(II)–O (Ba(II)–O).

Thirdly, for a given emitting ion, long decay time is characteristic of the most symmetrical surrounding while short decay values are observed when site distortion occurs [20]. According to Fig. 6, the $^5D_0$ decay time in Eu(I) and Eu(II) site is 2.31 ms and 2.01 ms at 10 K, respectively. It is obviously found that the lifetimes in Eu(I) site are longer than that in Eu(II) site. So Eu(I) site has more symmetrical surrounding than Eu(II) site. In addition, the decay curves of two $Eu^{3+}$ sites are single exponential, and the energy could not be transferred between Eu(I) and Eu(II) site. This is because Ba(I) and Y(Ba(II)) are along the a axis and the distance between them is very long, i.e. the distance between different $Eu^{3+}$ ions is quite long too.

As discussed above, it could be proposed that $Eu^{3+}$ ions occupy preferably the $Ba^{2+}$ sites. The required charge compensations for the occupation of $Eu^{3+}$ ions could be more complicated. This can most probably be achieved by the possible mechanism: the positive charge due to $Eu^{3+}$ ion substitute for $Ba^{2+}$ may be combined with the cation vacancy to form the dipole complexes of $[2(Eu_{Ba}{}^{3+})^{\bullet} - V_{Ba}{}'']$ and $[(Eu_{Ba}{}^{3+})^{\bullet} - V_{Na}{}']$. Such a charge compensation mechanism is very common in other components, e.g., $RE^{3+}$ doped apatite structure phosphate [22]. The possible negative charge compensation related to interstitial oxygen $O_i''$ here is difficult because this mechanism usually occurs in the case of the heavily RE-doping. And usually, in oxides, the reaction energy to create the $O_i''$ is higher than that of cation vacancy [23]. However, the defect compensation does not exert any obvious inuence on the luminescence of $Eu^{3+}$ in this sample because of the low doping level. This is in agreement with the excitation spectrum of $Eu^{3+}$ ions in Fig. 4, which presents that there is two $Eu^{3+}$ crystallographic site ascribed to have two occupancy sites of $Ba^{2+}$ in $NaBaPO_4$ lattice.

## 5. Conclusion

A red-emitting phosphor, $Eu^{3+}$-doped $NaBaPO_4$, was prepared by a general high-temperature solid-state reaction. Structural characterizations reveal that the phosphor derives from glaserite structure with space group $P\bar{3}m1$. The excitation spectrum consists of the strong f–f transitions of $Eu^{3+}$ ions, indicating $NaBaPO_4$: $Eu^{3+}$ can be efficiently excited by the radiation of near UV-emitting InGaN based LED chips. Under the near UV excitation the phosphor shows intense orange-red emission from the electric dipole transition $^5D_0 \rightarrow {}^7F_1$. The excitation spectrum corresponding to the $^7F_0 \rightarrow {}^5D_0$ transition consists of the strongest line at 579.6 nm Eu(I) and a weak peak at 578.9 nm Eu(II), indicating the $Eu^{3+}$ ions occupy two different crystallographic sites of $Ba^{2+}$ ions, i.e. the $Eu^{3+}$ ions occupy one intrinsic crystallographic site of Ba(I) and a probable site of Ba(II) or (Y) in $NaBaPO_4$ lattice.

## Acknowledgments

This work was supported by Program for Postgraduates Research Innovation in University of Jiangsu Province (2010) in China, and by Mid-career Researcher Program through National Research Foundation (NRF) grant funded by the Ministry of Education, Science and Technology (MEST) (Project No. 2009-0078682).

## References

[1] G. Blasse, A. Bril, W.-C. Nieuwpoort, On the $Eu^{3+}$ fluorescence in mixed metal oxides. Part I. The crystal structure sensitivity of the intensity ratio of electric and magnetic dipole emission, J. Phys. Chem. Solids 27 (1966) 1587–1592.

[2] C. Görller-Walrand, K. Binnemans, Rationalization of crystal-field parametrization, in: K.A. Gschneidner, Jr., L. Eyring (Eds.), Handbook on the Physics and Chemistry of Rare Earths, vol. 23, Elsevier Science, Amsterdam, 1996, pp. 121–283.

[3] W.R. Liu, C.C. Lin, Y.C. Chiu, Y.T. Yeh, S.M. Jang, R.S. Liu, $ZnB_2O_4$:$Bi^{3+}$, $Eu^{3+}$: a highly efficient, red-emitting phosphor, Opt. Express 18 (2010) 2946–2951.

[4] R.M. Krsmanović, Ž. Antić, M.G. Nikolić, M. Mitrić, M.D. Dramićanin, Preparation of $Y_2O_3$:$Eu^{3+}$ nanopowders via polymer complex solution method and luminescence properties of the sintered ceramics, Ceram. Int. 37 (2011) 525–531.

[5] K. Park, S.W. Nam, M.H. Heo, VUV photoluminescence properties of $Y_{1-x}Gd_xVO_4$:Eu phosphors prepared by ultrasonic spray pyrolysis, Ceram. Int. 36 (2010) 1541–1544.

[6] Y. Yu, D. Chen, P. Huang, H. Lin, Y. Wang, Structure and luminescence of $Eu^{3+}$ doped glass ceramics embedding ZnO quantum dots, Ceram. Int. 36 (2010) 1091–1094.

[7] G. Bhaskar Kumar, S. Buddhudu, Synthesis and emission analysis of $RE^{3+}$ ($Eu^{3+}$ or $Dy^{3+}$):$Li_2TiO_3$ ceramics, Ceram. Int. 35 (2009) 521–525.

[8] M.H. Hwang, Y.J. Kim, Luminescent properties of $Eu^{3+}$-doped $YTaO_4$ powders, Ceram. Int. 34 (2008) 1117–1120.

[9] R.Y. Yang, H.Y. Chen, C.M. Hsiung, S.J. Chang, Crystalline morphology and photoluminescent properties of $YInGe_2O_7$:$Eu^{3+}$ phosphors prepared from microwave and conventional sintering, Ceram. Int. 37 (2011) 749–752.

[10] S.-S. Chang, M.S. Jo, Luminescence properties of Eu-doped $SnO_2$, Ceram. Int. 33 (2007) 511–514.

[11] L. Elammari, M.E. Koumiri, I. Zschokke-Gränacher, B. Elouadi, Elaboration and non linear properties of orthophosphate solid solutions $A^IB^{II}{}_{1-x}M^{II}{}_xPO_4$ ($A^I$ = monovalent cation, $B^{II}$&$M^{II}$ = divalent cations), Ferroelectrics 158 (1994) 19–24.

[12] C.C. Lin, Z.R. Xiao, G.Y. Guo, T.S. Chan, R.S. Liu, Versatile phosphate phosphors $ABPO_4$ in white light-emitting diodes: collocated characteristic analysis and theoretical calculations, J. Am. Chem. Soc. 132 (2010) 3020–3028.

[13] W.J. Tang, D.H. Chen, Photoluminescent properties of $A$$BaPO_4$:Eu ($A$ = Na, K) phosphors prepared by the combustion-assisted synthesis method, J. Am. Ceram. Soc. 92 (2009) 1059–1061.

[14] X. Li, G. Li, X.N. Li, J.W. Wen, Z.P. Yang, Luminescent properties of $NaBaPO_4$:$Eu^{3+}$ red-emitting phosphor for white light-emitting diodes, Powder Technol. 200 (2010) 12–15.

[15] Z.J. Wang, Z.P. Yang, Q.L. Guo, P.L. Li, Preparation and luminescent characteristics of the $NaBaPO_4$:$Tb^{3+}$ green phosphor, Acta Phys. Chim. Sin. 26 (2010) 3317–3321.

[16] S.V. Upadeo, S.V. Moharil, Radiation-induced valence changes in Eu-doped phosphors, J. Phys.: Condens. Matter 9 (1997) 735–746.

[17] C. Alvo, R. Faggia, Crystal structure of the glaserite form of $BaNaPO_4$, Can. J. Chem. 53 (1975) 1849–1853.

[18] A.W. Kolsi, M. Quarton, W. Freundlich, Structure crystalline de $NaBaPO_4$, J. Solid State Chem. 36 (1981) 107–111.

[19] G. Blasse, The $Eu^{3+}$ luminescence as a measure for chemical bond differences in solids, Chem. Phys. Lett. 20 (1973) 573–574.

[20] R.A. Benhamou, A. Bessière, G. Wallez, B. Viana, M. Elaatmani, M. Daoud, A. Zegzouti, New insight in the structure–luminescence relationships of $Ca_9Eu(PO_4)_7$, J. Solid State Chem. 182 (2009) 2319–2325.

[21] F. Auzel, O. Malta, A scalar crystal-field strength parameter for rare earth ions: meaning and usefulness, J. Phys. 44 (1983) 201–206.

[22] M. Karbowiak, S. Hubert, Site-selective emission spectra of $Eu^{3+}$:$Ca_5(PO_4)_3F$, J. Alloys Compd. 302 (2000) 87–93.

[23] Q. Lin, X. Feng, Computer simulation study of extrinsic defects in $PbWO_4$ crystals, J. Phys.: Condens. Matter 15 (2003) 1963–1973.